Progress In Electromagnetics Research M, Vol. 23, 139–152, 2012

IMPROVED NUMERICAL METHOD FOR COMPUTING INTERNAL IMPEDANCE OF A RECTANGULAR CONDUCTOR AND DISCUSSIONS OF ITS HIGH FREQUENCY BEHAVIOR

M. Matsuki and A. Matsushima*

Graduate School of Science and Technology, Kumamoto University, 2-39-1 Kurokami, Kumamoto 860-8555, Japan

Abstract—An efficient numerical solution is been developed to compute the impedances of rectangular transmission lines. Method of moments is applied to integral equations for the current density, where the cross section is discretized, to improve the convergence, by a nonuniform grid that obeys the skin effect. Powerfulness of this approach up to rather high frequencies is verified by comparing with asymptotic formulas and other references. Detailed discussion is given for the current density distribution and its effect to the impedance, especially for a high frequency range.

1. INTRODUCTION

Transmission lines having conductors of rectangular cross section are typically found in MMIC [1, 2], and lots of formulas for the characteristic impedance and the attenuation coefficients have been proposed and collected [3, 4]. In the recent trend of high speed digital signal processing, the increase in the per-unit-length resistance and inductance due to the skin effect has become an issue of great interest. This problem, especially for a free-standing rectangular conductor as a basic structure, has been discussed from the viewpoints of analytical treatment [5–9], experiment [10], and numerical computation [11–17].

The classical approach based on the conformal mapping and perturbation [5–7] predicts the high frequency asymptotic behavior of the per-unit-length resistance in terms of the surface resistance and the complete elliptic integrals in the exact manner. Full-range

Received 21 December 2011, Accepted 23 January 2012, Scheduled 1 February 2012
* Corresponding author: Akira Matsushima (matsua@cs.kumamoto-u.ac.jp).

solution is attainable only by proper numerical techniques, and some of them [2, 12, 15, 16] discussed the accuracy of the obtained impedance values when the skin depth is much smaller than the line thickness. Nevertheless, it would seem that no attempt has been made to bridge the above mentioned analytical and numerical results. Besides, the series solution in [9] based on the Dirichlet boundary condition cannot incorporate the singular behavior of the current density at four corners.

Taking account of the above aspects, we first improve the computational method for the internal impedance of a rectangular conductor, and next give a circumstantial discussion about its high frequency behavior by comparing with analytical solutions. The integral equation for the current density in the cross section is solved by the method of moments [18]. Unlike the present author's approach [19], where the line is replaced by a set of round wires and the current is expanded by cylindrical functions, we here utilize simple rectangular segments and a constant basis. This process is, in principle, similar to that employed in [2, 13–15, 17], and among them, [15] proposed the use of a nonuniform grid without detailed explanation. The present paper, however, describes how to construct such grids systematically in accordance with the skin effect. The effectiveness of this treatment is demonstrated by numerical experiments. Referring to the perturbation solution [5–7] and the fitted formula [8], we gain new insights into the high frequency properties of the impedance and current density distribution.

2. NUMERICAL METHOD

2.1. Integral Equations

As shown in Figure 1, a conductor transmission line with rectangular cross section is free-standing in the vacuum. The cross section of the line is expressed by $S = \{\mathbf{r}(= \mathbf{i}_x x + \mathbf{i}_y y) | 0 < x < w,\ 0 < y < t\}$, where

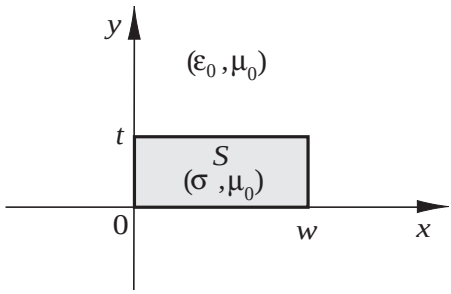

Figure 1. Rectangular conductor line in the vacuum.

$\mathbf{i}_x$ and $\mathbf{i}_y$ are the unit vectors in each direction. The conductivity of the line is σ, and the permittivity of the vacuum is ε_0. The line is assumed to be nonmagnetic, and so the permeability is μ_0 everywhere. The permittivity of the line is not taken into account, because we deal with the metal line where the displacement current is neglected.

Suppose that the current density $\mathbf{J}(\mathbf{r})$ in the line has only the axial component J_z. Then the vector potential $\mathbf{A}(\mathbf{r})$ has the same component which satisfies the Helmholtz equation in the vacuum

$$\left(\frac{\partial^2}{\partial x^2}+\frac{\partial^2}{\partial y^2}+\beta_0^2\right)A_z(\mathbf{r})=0, \quad \beta_0^2=\omega^2\varepsilon_0\mu_0 \tag{1}$$

Under the time factor $e^{j\omega t}$, the solution of (1) is written in terms of the Hankel function of the second kind as

$$A_z(\mathbf{r})=\frac{\mu_0}{4j}\int_{S\cup S_r} J_z(\mathbf{r}')\,H_0^{(2)}(\beta_0|\mathbf{r}-\mathbf{r}'|)\,dS' \tag{2}$$

where $\mathbf{r}'=\mathbf{i}_x x'+\mathbf{i}_y y'$, $dS'=dx'\,dy'$, and S_r is the cross section in which the return current flows. Let us fix S_r at such a far position that the signal current is not affected by it. We also assume that $|\mathbf{r}|$ is much smaller than the vacuum wavelength $2\pi/\beta_0$. This situation allows us to replace $H_0^{(2)}(\beta_0|\mathbf{r}-\mathbf{r}'|)$ with $(-2j/\pi)(\log|\mathbf{r}-\mathbf{r}'|+C_0)$ (C_0 : constant) and $H_0^{(2)}(\beta_0|\mathbf{r}'|)$ for S and S_r, respectively. Then we have

$$A_z(\mathbf{r})\approx-\frac{\mu_0}{2\pi}\left(\int_S J_z(\mathbf{r}')\log|\mathbf{r}-\mathbf{r}'|\,dS'+IC_0+C_r\right) \tag{3}$$

where the total current I and the constant C_r are written as

$$I=\int_S J_z(\mathbf{r}')\,dS', \quad C_r=\frac{j\pi}{2}\int_{S_r} J_z(\mathbf{r}')\,H_0^{(2)}(\beta_0|\mathbf{r}'|)\,dS' \tag{4}$$

Employing the relations concerning the electric field that $\mathbf{E}=-j\omega\mathbf{A}-\nabla\phi=\mathbf{J}/\sigma$, with ϕ being a scalar potential, we are led to the set of integral equations for the current density as

$$J_z(\mathbf{r})-\frac{j}{\pi\delta^2}\int_S J_z(\mathbf{r}')\,\log|\mathbf{r}-\mathbf{r}'|\,dS'=C \quad (\mathbf{r}\in S) \tag{5}$$

where $\delta=\sqrt{2/(\omega\mu_0\sigma)}$ is the skin depth of the metal, and $C=-\sigma(\partial\phi/\partial z)_S+j(IC_0+C_r)/(\pi\delta^2)$ is unknown constant.

2.2. Method of Moments

Let us discretize (5) by the method of moments [19], where two dimensional rectangular pulse functions are used for both basis and weighting functions [15, 17].

First, we slice the cross section S by $M+1$ horizontal lines and $N+1$ vertical lines

$$\begin{cases} x = x_0(=0), & x_1, & \ldots, & x_m, & \ldots, & x_{M-1}, & x_M(=w) \\ y = y_0(=0), & y_1, & \ldots, & y_n, & \ldots, & y_{N-1}, & y_N(=t) \end{cases} \tag{6}$$

such that $S = \bigcup_{m=1}^{M} \bigcup_{n=1}^{N} S_{mn}$ with $S_{mn} = \{\mathbf{r} | x_{m-1} < x < x_m,\, y_{n-1} < y < y_n\}$. The subsection S_{mn} has the area $\Delta S_{mn} = \Delta w_m \Delta t_n$, where $\Delta w_m = x_m - x_{m-1}$ and $\Delta t_n = y_n - y_{n-1}$.

Next, the current density J_z is approximated by a constant J_{mn} in S_{mn}. This procedure leads us to the set of linear relations

$$J_{mn} + \sum_{m'=1}^{M} \sum_{n'=1}^{N} G_{mn,m'n'} J_{m'n'} = C \quad \begin{pmatrix} m = 1, 2, \ldots, M; \\ n = 1, 2, \ldots, N \end{pmatrix} \tag{7}$$

where

$$G_{mn,m'n'} = \frac{\Delta S_{m'n'}}{j\pi\delta^2} \log R_{mn,m'n'} \tag{8}$$

and the symbol $R_{mn,m'n'}$ is a geometrical mean distance (GMD) between S_{mn} and $S_{m'n'}$ defined by

$$\log R_{mn,m'n'} = \frac{1}{\Delta S_{mn} \Delta S_{m'n'}} \int_{S_{mn}} \int_{S_{m'n'}} \log |\mathbf{r} - \mathbf{r}'| \, dS' \, dS \tag{9}$$

The analytical expression of GMD is given in [20, 15].

Since the constant C in (7) is unknown, one condition is lacking. This is supplemented by discretizing the former expression in (4) as

$$\sum_{m=1}^{M} \sum_{n=1}^{N} J_{mn} \Delta S_{mn} = I \tag{10}$$

where I is a preset constant. Equations (7) and (10) are altogether solved numerically for $MN+1$ unknowns J_{mn} and C.

2.3. Impedance Calculation

The per-unit-length resistance and internal inductance of the line are obtained in terms of Joule heat and stored magnetic energy, respectively. They are written as

$$R = \frac{1}{\sigma |I|^2} \int_S |\mathbf{J}(\mathbf{r})|^2 \, dS \approx \frac{1}{\sigma |I|^2} \sum_{m=1}^{M} \sum_{n=1}^{N} |J_{mn}|^2 \Delta S_{mn} \tag{11}$$

$$L^{in} = \frac{\mu_0}{|I|^2} \int_S |\mathbf{H}(\mathbf{r})|^2 \, dS \approx \frac{\mu_0}{|I|^2} \sum_{m=1}^{M} \sum_{n=1}^{N} |\mathbf{H}(\bar{\mathbf{r}}_{mn})|^2 \Delta S_{mn} \tag{12}$$

where $\bar{\mathbf{r}}_{mn}$ $(= \mathbf{i}_x \bar{x}_m + \mathbf{i}_y \bar{y}_n)$ is the midpoint of S_{mn} such that $\bar{x}_m = (x_m + x_{m-1})/2$ and $\bar{y}_n = (y_n + y_{n-1})/2$.

The magnetic field in (12) can be computed by applying (3) into $\mathbf{H} = (1/\mu_0)\nabla \times \mathbf{A}$ as

$$\begin{aligned}\mathbf{H}(\mathbf{r}) \;=\; & \frac{1}{2\pi} \sum_{m=1}^{M} \sum_{n=1}^{N} J_{mn} \left[-\mathbf{i}_x K(\Delta t_n, \Delta w_m, y - y_n, x - x_m) \right. \\ & \left. + \mathbf{i}_y K(\Delta w_m, \Delta t_n, x - x_m, y - y_n) \right] \end{aligned} \tag{13}$$

where the double integral

$$K(a, b, x, y) = \int_{-b/2}^{b/2} \int_{-a/2}^{a/2} \frac{x - x'}{(x - x')^2 + (y - y')^2} \, dx' \, dy' \tag{14}$$

is evaluated analytically as described in Appendix A.

3. NUMERICAL RESULTS

3.1. Convergence

Let us develop an effective solution to the integral equation by contriving computational grids as follows.

Uniform grid The simplest way is to fix as $\Delta w_m = \Delta w = w/M$ and $\Delta t_n = \Delta t = t/N$ with keeping $M/N \approx w/t$, which gives $x_m = m\Delta w$ and $y_n = n\Delta t$. But this is ineffective at high frequencies where the skin effect becomes prominent.

Nonuniform grid Better convergence is expected if we let the segments smaller near the conductor surface than at the center. Accordingly, let us set the position of the nodes x_m by the rule

$$\frac{m}{M} = \int_0^{x_m} |g_w(x)| \, dx \Big/ \int_0^{w} |g_w(x)| \, dx \quad (m = 0, 1, \ldots, M) \tag{15}$$

where the function simulating the current behavior is

$$g_w(x) = \cosh \frac{(1 + j)(x - w/2)}{\delta} \Big/ \cosh \frac{(1 + j)w}{2\delta} \tag{16}$$

so that $g_w(0) = g_w(w) = 1$. Its amplitude in the high frequency region is approximated as

$$|g_w(x)| \approx \cosh \frac{x - w/2}{\delta} \Big/ \cosh \frac{w}{2\delta} \quad (\delta \ll w) \tag{17}$$

Solving (15) and (17) leads us to

$$x_m = \frac{w}{2} + \delta \operatorname{arcsinh} \left[\frac{2m - M}{M} \sinh \frac{w}{2\delta} \right] \tag{18}$$

Similar procedure gives us the node y_n in the form analogous to (18), with w, m, and M replaced by t, n, and N, respectively. The balance of the truncation numbers is kept by

$$\frac{M}{N} \approx \frac{\displaystyle\int_0^w |g_w(x)|\,dx}{\displaystyle\int_0^t |g_t(y)|\,dy} = \frac{\tanh\dfrac{w}{2\delta}}{\tanh\dfrac{t}{2\delta}} \tag{19}$$

Figure 2 shows the examples of grid at middle and high frequencies f $(= \omega/(2\pi))$. Note that the skin depth δ is 20.9 μm and 2.1 μm at 10 MHz and 1000 MHz, respectively. In Figure 2(a), δ and t are comparable so that $M > N$. However, in Figure 2(b), the ratio $\delta/t = 0.09$ is so small that the criterion (19) predicts $M = N$ even for the rectangular cross section.

Figure 3 shows the real and imaginary parts of the line impedance computed from (7) and (10) as a function of the truncation number

f = 10 MHz, M = 7, N = 3 (a)

f = 1000 MHz, M = 7, N = 7 (b)

Figure 2. Grid for $w = 5t = 111.8\,\mu\text{m}$ and $\sigma = 58\,\text{MS/m}$.

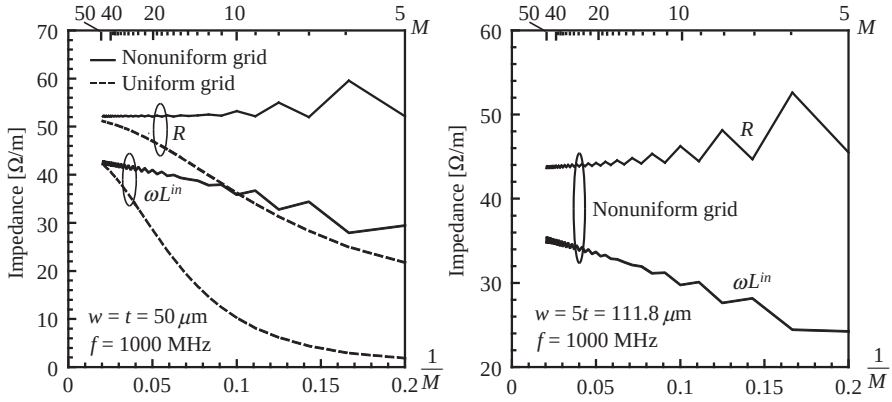

Figure 3. Convergence of per-unit-length impedance for copper lines having common parameters $wt = 2500\,\mu\text{m}^2$ and $\sigma = 58\,\text{MS/m}$. (a) Square line. (b) Rectangular line.

M. The converged values of R and ωL^{in} are found by extrapolating the curves up to the vertical axis where $M \to \infty$. Though the sectional area wt is common, the resistance R converges to different values, $52\,\Omega$/m and $43\,\Omega$/m, for Figures 3(a) and (b), respectively. This difference stems from the fact that, at high frequencies, R is inversely proportional to the perimeter $2(w+t)$ at a rough guess. Comparison of the solid and broken lines in Figure 3(a) reveals the effectiveness of using the nonuniform grid shown in Figure 2. There are two independent series for odd M and even M, and the former exhibits better convergence.

3.2. Frequency Characteristics

Figure 4 shows the frequency dependence of the impedance compared with other solutions. Under the fixed cross section wt, the ratio w/t is chosen as 1 (square), 5, and 10 for Figures 4(a), (b), and (c), respectively. The solid curves are the numerical solution to the linear Equations (7) and (10). The resistance R and reactance ωL^{in} behave as $O(f^0)$ and $O(f^1)$, respectively, at low frequencies, whereas, they shift to the same order $O(f^{1/2})$ as frequency increases. The curves for R agree well with the open circles based on the previous reports [15, 8]. In [15] the method of moments similar to ours is used, and in [8] the expression

$$\frac{R}{R_{dc}} = \begin{cases} \dfrac{0.43093x_w}{1+0.041(w/t)^{1.19}} + \dfrac{1.1147+1.2868x_w}{1.2296+1.287x_w^3} & (x_w \geq x_{w0}) \\ +0.0035(w/t-1)^{1.8} & \\ 1+0.0122x_w^{3+0.01x_w^2} & (x_w < x_{w0}) \end{cases} \tag{20}$$

is proposed by fitting the measured values in [10]. Here, the dc resistance, the parameter x_w, and its boundary are

$$R_{dc} = \frac{1}{\sigma wt}, \quad x_w = \sqrt{\frac{2}{\pi}} \cdot \frac{\sqrt{wt}}{\delta}, \quad x_{w0} = 2.5 \tag{21}$$

The crossover frequency corresponding to $x_w = 2.5$ is 17.1 MHz, beside which the sequence of circles exhibits a slight discontinuity in Figures 4(b) and (c) due to the separate expressions in (20). These could be smoothly bridged by choosing the boundary x_{w0} not as constant 2.5 but as

$$x_{w0} = \begin{cases} 4.5 - 1.4\sqrt{w/t} & (1 < w/t < 4) \\ 1.7 & (4 < w/t < 9) \\ -0.1 + 0.6\sqrt{w/t} & (9 < w/t < 16) \end{cases} \tag{22}$$

which varies between 1.7 and 3.1.

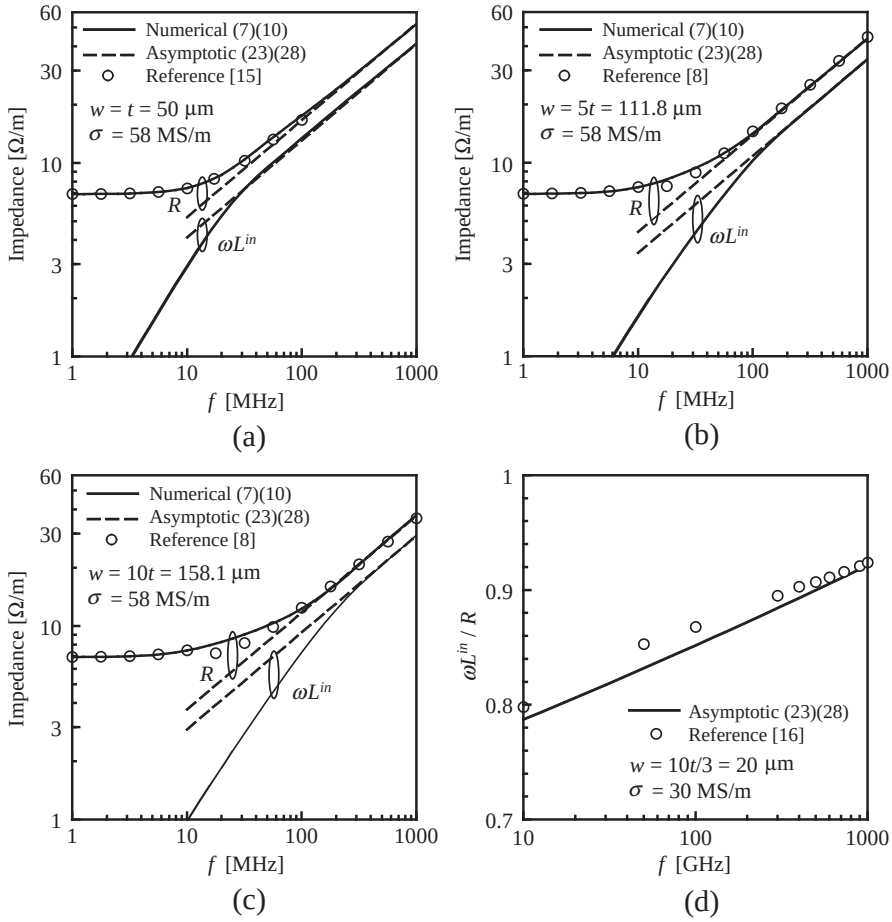

Figure 4. Frequency dependence of the per-unit-length impedance. The parameters wt and σ are common to (a), (b), and (c). (a) $w/t = 1$. (b) $w/t = 5$. (c) $w/t = 10$. (d) Ratio of reactance to resistance for $w/t = 10/3$. In [16], the line is put on a dielectric substrate and is surrounded by an enclosure made of electric and magnetic walls.

Let us shift our subject to the high frequency behavior in Figure 4. It is well known that the conductor with circular cross section has the property that the ratio $\omega L^{in}/R \to 1$ as $f \to \infty$. This is not the case, however, for rectangular lines, and discussions about the behavior of $\omega L^{in}/R$ have ever occurred [9, 15, 16]. It deserves to reconsider this problem, and therefore, we quote the following asymptotic expressions for R and ωL^{in}.

Resistance The charge distribution on the conductor surface is

derived by the conformal mapping method for the static case. Introduction of the surface resistance $R_s = 1/(\sigma\delta)$ allows us to write the formula as [5–7]

$$R = \frac{2R_s}{\pi^2\sqrt{wt}} \sqrt{[E(\kappa) - \tilde{\kappa}^2 K(\kappa)][E(\tilde{\kappa}) - \kappa^2 K(\tilde{\kappa})]}\ [K(\kappa) + K(\tilde{\kappa})] \tag{23}$$

where $K(\cdot)$ and $E(\cdot)$ are the complete elliptic integrals of the first kind and second kind, respectively, and $\tilde{\kappa} = \sqrt{1-\kappa^2}$. The value of κ is a solution of

$$t/w = \left[E(\kappa) - \tilde{\kappa}^2 K(\kappa)\right] / \left[E(\tilde{\kappa}) - \kappa^2 K(\tilde{\kappa})\right] \tag{24}$$

In the special case where $w = t$, we have $\kappa^2 = \tilde{\kappa}^2 = 0.5$ and $R = R_s/(\pi w)$.

Internal inductance We intentionally model the magnetic field as

$$\mathbf{H}(\mathbf{r}) \approx \frac{I}{2(w+t)} \left[-h_t(y)\mathbf{i}_x + h_w(x)\mathbf{i}_y\right] \quad (\mathbf{r} \in S) \tag{25}$$

circulating inside S, where

$$h_w(x) = \sinh\frac{(1+j)(x-w/2)}{\delta} \Big/ \sinh\frac{(1+j)w}{2\delta} \tag{26}$$

so that $h_w(0) = h_w(w) = 1$. Using $\mathbf{J} = \nabla \times \mathbf{H}$, we can confirm that (4) is satisfied if $w, t \gg \delta$. Substituting (25) into (12) and employing the high frequency expression of $|h_w(x)|$ similar to (17), we are led to the asymptotic formula

$$\omega L^{in} \approx \frac{R_s}{2(w+t)} = \frac{1}{2(w+t)} \sqrt{\frac{\pi\mu_0 f}{\sigma}} \tag{27}$$

This gives rather accurate values if $w = t$, but this is not necessarily the case for rectangular cross sections because of the different field distribution near the longer and shorter sides. Via numerical experiment, we improve the accuracy by modifying the frequency dependence as

$$\omega L^{in} \approx \frac{1}{2(w+t)} \sqrt{\frac{\pi\mu_0 f_0}{\sigma} \left(\frac{f}{f_0}\right)^{(w/t)^{0.05}}} \quad (w \geq t) \tag{28}$$

with the reference frequency $f_0 = 19/(\pi\mu_0\sigma w^{0.5} t^{1.5})$.

In Figures 4(a)–(c), we find that the results by the asymptotic formulas (23) and (28) approach the present numerical solution of (7) and (10) as frequency is increased. Agreement is observed roughly as $f > 200\,\mathrm{MHz}$ corresponding to $\delta/\sqrt{wt} < 1/10$. Figure 4(d)

demonstrates the validity of the asymptotic formulas by comparison with the full-wave mode matching approach in [16]. Even at $f = 1000\,\mathrm{GHz}$ that corresponds to $\delta/t \approx 1/100$, the ratio $\omega L^{in}/R$ amounts to 0.9 and is far from 1. Note that, though the geometries are not exactly the same, such a comparison still makes sense. This is because the ratio $\omega L^{in}/R$ is considered to be rather insensitive to the width of enclosure (now $w + 2s = 35\,\mu\mathrm{m}$) introduced in [16]. In fact, as shown in Figure 5 of [18], the proximity effect due to the electric walls and line images adds to R and L^{in} in similar extent. Besides, the existence of dielectric substrate does not affect the pattern of the magnetic field.

3.3. Current Behavior

Figure 5 shows the current density distribution in the square cross section at a medium frequency such that $w = t = 5.4\delta$. The density $J_z(x, y)$, normalized by the dc value I/wt, are displayed by contour lines. The skin and edge effects are discussed as below.

- Figure 5(a) is based on the numerical solution of (7) and (10). The contours are close to concentric circles and the current concentrate into four corners with the maximum value 3.5. The impedance is $12.7 + j9.5\,\Omega/\mathrm{m}$. The shapes and arrangement of contour lines resemble those of Figure 3(b) in [12].
- It is meaningful to mention the analytical solution under the Dirichlet boundary condition [9]. A constant voltage source is impressed over the rectangular surface, by which the per-unit-length impedance and the internal electric fields are obtained as the series expressions (10) and (15) in [9], respectively. As shown in Figure 5(b), this boundary condition gives constant current density 2.1 along the profile. Though this approach works for the circular cross section, it fails to take into account the edge effect of rectangular conductors. This is why the impedance, $11.6 + j9.0\,\Omega/\mathrm{m}$, is a little lower than that of Figure 5(a).
- To give suggestive information, we take up the plausibility of (25) representing the magnetic field $\mathbf{H}$. Figure 5(c), drawn by $\mathbf{J} = \nabla \times \mathbf{H}$ combined with (25), clearly represents the edge effect. The definition of resistance (11) leads us to

$$R \approx \omega L^{in} + \frac{2}{\sigma(w + t)^2} \tag{29}$$

  with ωL^{in} given in (27). The impedance $12.6 + j9.3\,\Omega/\mathrm{m}$ is comparable to that of Figure 5(a). Note that this approach gives rather accurate internal inductance as $f \geq 50\,\mathrm{MHz}$, but that the resistance at 1000 MHz is underestimated by 14% compared with

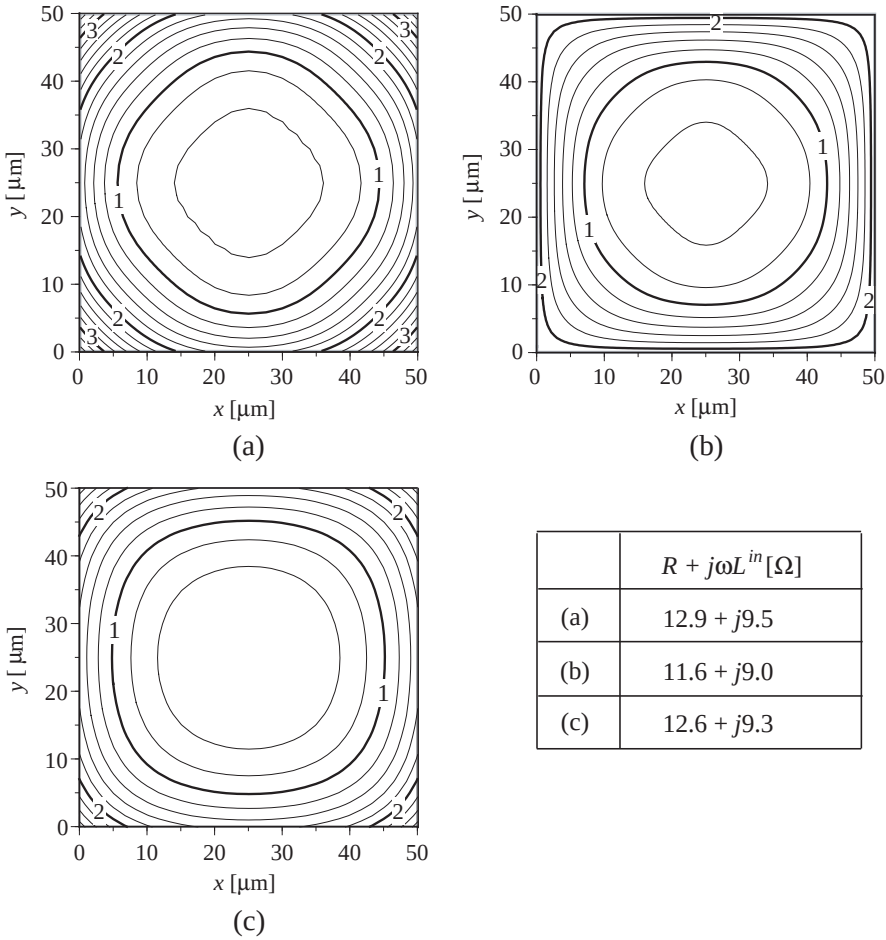

	$R + j\omega L^{in}$ [Ω]
(a)	12.9 + *j*9.5
(b)	11.6 + *j*9.0
(c)	12.6 + *j*9.3

Figure 5. Normalized current density $|wtJ_z(x,y)/I|$ for $w = t = 50\,\mu\text{m}$, $\sigma = 58\,\text{MS/m}$ and $f = 50\,\text{MHz}$. (a) Present numerical solution of (7) and (10). (b) Based on the Dirichlet boundary condition [9]. (c) Based on the approximate magnetic field (25).

the numerical result. Needless to say, the above discussion holds only for the square cross section.

After the manner of [2] and [12], we evaluate the coefficient k which indicates how the current concentrates into the conductor surface. The results are listed in Table 1 for several values of w/t and $2\delta/t$. The value of k is defined as follows. As in Figure 4.23 in [2] or Figure 10 in [12], we suppose that the current flows uniformly along the conductor surface

Table 1. Coefficient $k = R_s/[R(w+t)]$ indicating the degree of concentration of the surface current.

Present solution

$2\delta/t$ \ w/t	1	2	4	8
1	0.96	1.17	1.20	1.17
0.5	1.40	1.43	1.41	1.32
0.25	1.50	1.49	1.43	1.32
+0	1.57	1.55	1.44	1.32

Reference [2]

$2\delta/t$ \ w/t	1	10.7
≤ 0.7		1.3
0.286	1.486	
0.264	1.58	

Reference [12]

$2\delta/t$ \ w/t	≤ 6
small	1.67

with the thickness $k\delta/2$. This estimates the approximate resistance as

$$R = \frac{1}{\sigma \cdot 2(w+t) \cdot (k\delta/2)} = \frac{R_s}{k(w+t)} \tag{30}$$

with $R_s = 1/(\sigma\delta)$ being the surface resistance. From (30) we have $k = R_s/[R(w+t)]$. In Table 1, the square case at $w/t = 1$ shows the largest variation in k according to the change of $2\delta/t$. This is because the current shifts from flat surfaces to separated four corners, making k unstable. Results in [2] and [12] are also tabulated, where k extends from 1.3 to 1.67 for several parameters (κ in [12] is about 1.2, which corresponds to $2/k$ in the present notation). The maximum values of k can be predicted by the asymptotic formula (23), and are given in the lowest row for $2\delta/t = +0$ in the present solution. If $w/t = 1$, (23) and (24) give the analytical result that $\kappa^2 = 0.5$, $R = R_s/(\pi w)$, and $k = \pi/2 = 1.57$. The data at $2\delta/t = +0$ are fitted by the formula

$$k = 1.57 - 0.06\,[\log(w/t)]^2 \tag{31}$$

the absolute error of which is less than 0.01.

Finally, in order to find out the relation between the independent descriptions in [2] and [8], let us examine the crossover frequency at which the resistance curve shifts from $O(f^0)$ to $O(f^{1/2})$. As done in [2], we set the high frequency resistance R in (30) equal to the dc value R_{dc} in (21), leading to $wt = k\delta(w+t)$. This equation is reduced to $w = \pi\delta$ if $w = t$ and $k = \pi/2$. Then the parameter x_w in (21) becomes $\sqrt{2\pi} \approx 2.5$ which agrees with the value proposed in [8].

4. CONCLUSION

The numerical solution has been developed to compute the impedances of rectangular transmission lines. Method of moments was applied to integral equations for the current density, where the cross section is discretized by a nonuniform grid to improve the numerical efficiency. Comparison with other data reveals the powerfulness of the present approach for wide frequency ranges. Special attention is paid to the current density distribution and its effect to the impedance. The present analysis can be readily extended to the cases where the number of conductor is increased or the conductors are attached on a lossy substrate. These problems deserve further treatment.

APPENDIX A. ANALYTICAL EXPRESSION OF (14)

The double integral (14) is evaluated as

$$K(a,b,x,y) = \sum_{\mu=0}^{1}\sum_{\nu=0}^{1}(-1)^{\mu+\nu}\tilde{K}\left(x+(-1)^{\mu}\frac{a}{2}, y+(-1)^{\nu}\frac{b}{2}\right) \quad \text{(A1)}$$

where

$$\tilde{K}(\alpha,\beta) = \int_0^{\beta}\int_0^{\alpha}\frac{\xi}{\xi^2+\eta^2}\,d\xi\,d\eta = \alpha\arctan\frac{\beta}{\alpha}+\frac{\beta}{2}\log\left(1+\frac{\alpha^2}{\beta^2}\right) \quad \text{(A2)}$$

REFERENCES

1. Edwards, T. C. and M. B. Steer, *Foundations of Interconnect and Microstrip Design,* 3rd edition, John Wiley & Sons, 2000.
2. Paul, C. R., *Analysis of Multiconductor Transmission Lines,* 2nd Edition, John Wiley & Sons, 2008.
3. Wadell, B. C., *Transmission Line Design Handbook*, Artech House, Boston, 1991.
4. Gunston, M. A. R., *Microwave Transmission Line Impedance Data,* Noble, Atlanta, 1996.
5. Cockcroft, J. D., "Skin effect in rectangular conductors at high frequencies," *Proc. Roy. Soc. London*, Vol. A122, 533–542, 1929.
6. Bickley, W. G., "Two-dimensional potential problems for the space outside a rectangle," *Proc. London Math. Soc.*, Ser. 2, Vol. 37, 82–105, 1932.
7. Flax, L. and J. H. Simmons, "Magnetic field outside perfect rectangular conductors," *NASA Technical Note*, No. NASA-TN-D-3572, 1–19, 1966.

8. Pettenpaul, E., H. Kapusta, A. Weisgerber, H. Mampe, J. Luginsland, and I. Wolff, "CAD models of lumped elements on GaAs up to 18 GHz," *IEEE Trans. Microwave Theory Tech.*, Vol. 36, No. 2, 294–304, 1988.
9. Rong, A. and A. C. Cangellaris, "Note on the definition and calculation of the per-unit-length internal impedance of a uniform conducting wire," *IEEE Trans. Electromag. Compat.*, Vol. 49, No. 3, 677–681, 2007.
10. Haefner, S. J., "Alternating current resistance of rectangular conductors'," *Proc. IRE*, Vol. 25, 434–447, 1937.
11. Weeks, W., L. Wu, M. McAllister, A. Singh, "Resistive and inductive skin effect in rectangular conductors," *IBM J. Res. Dev.*, Vol. 23, No. 6, 652–660, 1979.
12. Faraji-Dana, R. and Y. Chow, "Edge condition of the field and AC resistance of a rectangular strip conductor'," *IEE Proc. H*, Vol. 137, No. 2, 133–140, 1990.
13. Barr, A. W., "Calculation of frequency-dependent impedance for conductors of rectangular cross section," *AMP J. Technol.*, Vol. 1, 91–100, 1991.
14. Sarkar, T. K. and A. R. Djordjević, "Wideband electromagnetic analysis of finite-conductivity cylinders," *Progress In Electromagnetics Research*, Vol. 16, 153–173, 1997.
15. Antonini, G., A. Orlandi, and C. R. Paul, "Internal impedance of conductors of rectangular cross section," *IEEE Trans. Microwave Theory Tech.*, Vol. 47, No. 7, 979–985, 1999.
16. Heinrich, W., "Comments on 'Internal impedance of conductors of rectangular cross section'," *IEEE Trans. Microwave Theory Tech.*, Vol. 49, No. 3, 580–581, 2001.
17. Berleze, S. L. M. and R. Robert, "Skin and proximity effects in nonmagnetic conductors," *IEEE Trans. Education*, Vol. 46, No. 3, 368–372, 2003.
18. Matsushima, A. and H. Sakamoto, "Application of wire model to calculation of impedance of transmission lines with arbitrary cross sections," *Electronics and Communication in Japan (Part II: Electronics)*, Vol. 85, No. 7, 1–10, 2002.
19. Harrington, R. F., *Field Computation by Moment Methods*, Macmillan, New York, 1968.
20. Higgins, T. J., "Formulas for the geometrical mean distance of rectangular areas and line segments," *Appl. Phys.*, Vol. 14, No. 2, 188–195, 1943.